

000 LUMINA[★]: DETECTING HALLUCINATIONS IN RAG 001 SYSTEM WITH CONTEXT–KNOWLEDGE SIGNALS 002

003 **Anonymous authors**
004

005 Paper under double-blind review
006

007 ABSTRACT 008

009 Retrieval-Augmented Generation (RAG) aims to mitigate hallucinations in large
010 language models (LLMs) by grounding responses in retrieved documents. Yet,
011 RAG-based LLMs still hallucinate even when provided with correct and sufficient
012 context. A growing line of work suggests that this stems from an imbalance be-
013 tween how models use external context and their internal knowledge, and several
014 approaches have attempted to quantify these signals for hallucination detection.
015 However, existing methods require extensive hyperparameter tuning, limiting their
016 generalizability. We propose LUMINA, a novel framework that detects halluci-
017 nations in RAG systems through *context–knowledge signals*: external context
018 utilization is quantified via distributional distance, while internal knowledge uti-
019 lization is measured by tracking how predicted tokens evolve across transformer
020 layers. We further introduce a framework for statistically validating these mea-
021 surements. Experiments on common RAG hallucination benchmarks and four
022 open-source LLMs show that LUMINA achieves consistently high AUROC and
023 AUPRC scores, outperforming prior utilization-based methods by up to +13%
024 AUROC on HalluRAG. Moreover, LUMINA remains robust under relaxed assump-
025 tions about retrieval quality and model matching, offering both effectiveness and
026 practicality.
027

028 1 INTRODUCTION 029

030 Large language models (LLMs) are prone to hallucination, *i.e.*, producing responses that are factually
031 incorrect, nonsensical, or not grounded in the input or available data, while still appearing fluent and
032 plausible (Luo et al., 2024; Huang et al., 2024; Park et al., 2025). One commonly used strategy to
033 mitigate hallucination is providing LLMs with relevant information retrieved from external knowledge
034 bases, so-called Retrieval-Augmented Generation (RAG) (Shuster et al., 2021; Fan et al., 2024; Gao
035 et al., 2024). However, despite having sufficient and relevant retrieved documents, RAG systems still
036 have a chance to hallucinate and produce statements that are either unsupported or contradict the
037 retrieved information (Niu et al., 2024; Ridder & Schilling, 2025).
038

039 Recent work has shown that such failures often arise from conflicts between an LLM’s internal
040 knowledge and the retrieved external context (Xu et al., 2024). In these cases, models tend to
041 over-rely on internal knowledge regardless of correctness, undermining factual reliability (Longpre
042 et al., 2021; Li et al., 2023; Sun et al., 2025a; Yamin et al., 2025). Inspired by this observation,
043 recent approaches attempt to quantify hallucinations in RAG (Sun et al., 2025b; Wang, 2025; Tao
044 et al., 2025). However, existing methods rely on mechanistic interpretability heuristics—such as
045 selecting specific attention heads or transformer layers to achieve the optimal hallucination detection
046 performance—which require heavy hyperparameter tuning and often fail to generalize across models
047 and datasets.
048

049 To overcome these limitations, we propose LUMINA, a new framework for detecting hallucinations in
050 RAG system through *context–knowledge signals*, namely the signals of external context utilization and
051 internal knowledge utilization, as shown in Figure 1. Rather than targeting particular attention heads
052 or layers, LUMINA measures these signals in a layer-agnostic manner, requiring less hyperparameter
053 tuning. Specifically, for **external context utilization**, we measure the discrepancy between predictive
distributions conditioned on retrieved documents *vs.* random documents. A larger discrepancy
indicates that the LLM is more sensitive to semantic changes in documents when generating the

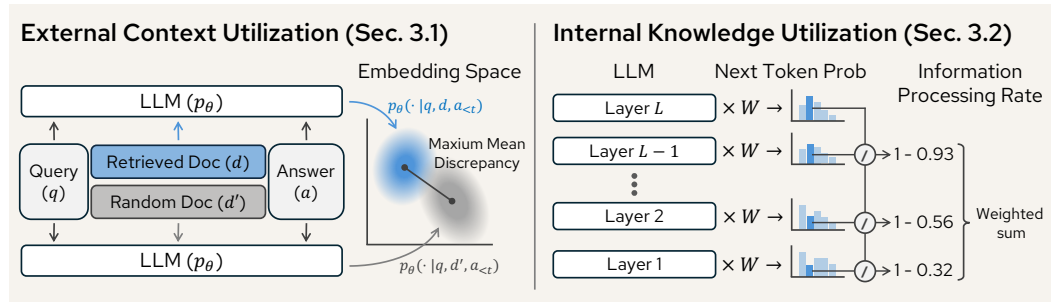


Figure 1: **The overview of LUMINA.** For external context utilization, we propose to measure the maximum mean discrepancy between two next token probability distributions conditioned on different documents. For internal knowledge utilization, we introduce the idea of information processing rate by looking at the ratio of the most probable output token’s probability across transformer layers and use it to determine the amount of utilized internal knowledge when generating the next token.

answer, implying higher reliance on the external context. For **internal knowledge utilization**, we track how the model’s internal states and token predictions evolve across layers: if the internal layers’ predictions do not converge to the final output until later layers, it suggests more information is added during the layer-wise process, implying stronger reliance on internal knowledge. We further validate the soundness of our measurements through statistical hypothesis testing on verifiable implications, establishing a stronger link between the proposed scores and actual utilization.

We conduct extensive experiments on common RAG hallucination benchmarks and across four LLMs to evaluate the performance of LUMINA on hallucination detection. The results show that the hallucination score calculated with LUMINA outperforms existing methods by a significant margin. For example, LUMINA achieves more than 0.9 AUROC on the HalluRAG datasets across models, with improvements of up to **+13%** over prior state-of-the-art. Importantly, the decomposition into external context utilization and internal knowledge utilization provides interpretable insights: hallucinations are strongly associated with low external context scores and disproportionately high internal knowledge scores. We further demonstrate that LUMINA is robust across different retrieval settings. These results validate both the effectiveness and practicality of our framework.

Our key contributions are summarized as follows:

1. We propose LUMINA, a novel approach to quantify utilization of external context and internal knowledge for RAG-based hallucination detection.
2. We propose a framework to statistically validate LUMINA, showing that they align with the intended results.
3. We conduct extensive experiments and show that LUMINA outperforms both score-based and learning based methods in hallucination detection, establishing new *state-of-the-art*.

2 PRELIMINARIES

2.1 PROBLEM FORMULATION AND MOTIVATION

RAG systems aim to improve factuality by incorporating external documents into the generation process. In cases such as news summarization, information extraction given a json file, and question answering that requires information emerging after the model’s release date, RAG is usually necessary because an LLM cannot rely solely on its internal knowledge to complete the task. However, in such cases, hallucinations still occur when a model over-relies on its internal parametric knowledge and under-utilizes the retrieved external context. We provide a formal definition below.

Conjecture 1 (External context vs. internal knowledge utilization). Let p_θ be an RAG-based LLM that takes a query q and retrieved documents d as inputs to generate a response a . Assume d is relevant to q and contains correct and sufficient information to respond to q . Denote $\mathcal{E}_{p_\theta}(a|q, d)$, $\mathcal{I}_{p_\theta}(a|q, d) \in \mathbb{R}$ be the signals of external context utilization and internal knowledge utilization of p_θ , respectively, when generating a . The response a is more likely to be hallucination if $\mathcal{I}_{p_\theta}(a|q, d) \gg \mathcal{E}_{p_\theta}(a|q, d)$.

108 Conjecture 1 is built on a principled intuition that, if a LLM requires external knowledge to complete
 109 a task and if a retriever can provide the LLM sufficient external information, the LLM should utilize
 110 those external context and ground its reasoning ability on those context. Therefore, a response in this
 111 scenario will be considered less reliable if it disproportionately relies on the LLM’s internal knowledge
 112 without a sufficient amount of external knowledge utilization.

113 **Definition 2.1 (Hallucination in an RAG system).** *Based on Conjecture 1, we define hallucination
 114 scores at both the token and response level. Specifically, for a generated answer $a = (a_1, \dots, a_T)$
 115 with T tokens, let $\mathcal{E}_{p_\theta}(a_t|q, d, a_{<t}), \mathcal{I}_{p_\theta}(a_t|q, d, a_{<t}) \in \mathbb{R}$ be the signals of external context utilization
 116 and internal knowledge utilization of p_θ when generating the token a_t , respectively. The token-level
 117 hallucination score of a_t is defined as*

$$\mathcal{H}_t(a_t|q, d, a_{<t}) := \lambda \cdot \mathcal{I}_{p_\theta}(a_t|q, d, a_{<t}) - (1 - \lambda) \cdot \mathcal{E}_{p_\theta}(a_t|q, d, a_{<t}), \quad (1)$$

120 where λ is a hyperparameter. Similarly, the response-level hallucination score of the response a is
 121 defined as the average of the token-level hallucination scores, i.e.,

$$\mathcal{H}_r(a|q, d) := \frac{1}{T} \sum_{t=1}^T \mathcal{H}_t(a_t|q, d, a_{<t}). \quad (2)$$

125 In this paper, we focus on the core question: **How to quantify the utilization of external context and
 126 internal knowledge?**

128 2.2 RELATED WORK

130 Prior works have attempted to quantify $\mathcal{E}_{p_\theta}(a_t|q, d, a_{<t})$ and $\mathcal{I}_{p_\theta}(a_t|q, d, a_{<t})$ using empirical met-
 131 rics (Sun et al., 2025b; Wang, 2025). For example, Sun et al. (2025b) proposed ReDeEP, which
 132 measures external context utilization through cosine similarity between the generated token and to-
 133 kens in context that have high attention weights w.r.t. certain attention heads. For internal knowledge
 134 utilization, it measures the Jensen-Shannon (JS) divergence between the hidden states before/after
 135 the FFN layer of certain transformer layers. The success of ReDeEP on some RAG hallucination
 136 detection datasets validates the idea of Conjecture 1. Wang (2025) combine the idea of ReDeEP with
 137 semantic entropy probes (SEP) (Han et al., 2024). They quantified external context utilization by
 138 measuring the semantic correlation between the semantic entropy of the generated token and attended
 139 tokens in the context. For internal knowledge utilization, they measured the absolute difference
 140 between the semantic entropy corresponding to hidden states before and after the FFN layer.

141 Although these approaches effectively detect hallucinations in the RAG system, they have two major
 142 limitations. First, these approaches require selecting specific attention heads and transformer layers
 143 to compute the external context score and internal knowledge score. However, the selection process
 144 is non-trivial and requires extensive hyperparameter tuning. In addition, these hyperparameters are
 145 dataset and model-specific, limiting the generalizability across different datasets and models. Another
 146 limitation is that although these works demonstrated the correlation between their proposed scores
 147 and hallucination, they did not validate whether the scores truly reflect the utilization of external
 148 context and internal knowledge.

149 3 METHODOLOGY

151 **Overview.** To overcome the limitations of prior empirical approaches, we introduce LUMINA, a new
 152 framework for quantifying both external context and internal knowledge utilization. In Section 3.1 and
 153 Section 3.2, we formalize the quantification of the two signals, which will be combined to compute
 154 the final hallucination score. In Section 3.3, we propose to validate the soundness of LUMINA through
 155 extensive hypothesis testing, addressing the challenges of score validation in previous works.

157 3.1 QUANTIFYING EXTERNAL CONTEXT UTILIZATION

159 To measure LLM’s external context utilization, our key idea is to assess its sensitivity to semantic
 160 changes in the input documents. If the LLM effectively incorporates the external context to generate
 161 a response, then replacing relevant documents with random ones should noticeably change the token
 162 probability distribution. Formally, we propose the following measurement:

162 **Measurement 1 (External context utilization).** Let a be an LLM-generated answer to query q
 163 with retrieved documents d as input. Assume d is relevant to q and contains correct and sufficient
 164 information to respond to q . Let d' be a subset of random documents irrelevant to q . The model's
 165 predictive distribution over tokens induces two (approximated) distributions over embeddings:
 166

$$P(E_v) = p_\theta(v | q, d, a_{<t}), \quad Q(E_v) = p_\theta(v | q, d', a_{<t}), \quad (3)$$

168 where each token $v \in \mathcal{V}$ in the vocabulary space is associated with an embedding $E_v \in \mathbb{R}^D$.
 169 Then, the degree to which the model uses external context for generating token a_t is reflected in the
 170 divergence between the two distributions conditioned on d versus d' :
 171

$$\mathcal{E}_{p_\theta}(a_t | q, d, a_{<t}) := \Delta(P, Q), \quad (4)$$

172 where $\Delta : \mathcal{P} \times \mathcal{P} \rightarrow \mathbb{R}_+$ is a distance function between two probability distributions.
 173

174 Note that we adopt $P(E_v)$ and $Q(E_v)$ as proxies to approximate the ground truth embedding
 175 distribution, as it is challenging to estimate it over the high-dimensional vector space. We instantiate
 176 Δ with Maximum Mean Discrepancy (MMD), which measures the distance of two probability
 177 distributions by mapping them into a Reproducing Kernel Hilbert Space.
 178

179 **Definition 3.1 (Maximum Mean Discrepancy)** (Gretton et al., 2012)). Given a positive semi-definite
 180 kernel function k , the squared MMD between two probability distributions P and Q is defined as
 181

$$\text{MMD}_k^2(P, Q) := \mathbb{E}_{\mathbf{A}, \mathbf{A}' \sim P}[k(\mathbf{A}, \mathbf{A}')] + \mathbb{E}_{\mathbf{B}, \mathbf{B}' \sim Q}[k(\mathbf{B}, \mathbf{B}')] - 2\mathbb{E}_{\mathbf{A} \sim P, \mathbf{B} \sim Q}[k(\mathbf{A}, \mathbf{B})], \quad (5)$$

182 where \mathbf{A}, \mathbf{A}' are i.i.d. vectors randomly sampled from P and \mathbf{B}, \mathbf{B}' are sampled from Q .
 183

184 This metric provides us with a non-parametric and LLM-agnostic way to quantify the utilization of
 185 external context, making it generalizable to different models and datasets.
 186

187 By rewriting MMD with P and Q we defined in Eq. (3) over token embeddings, we obtain:
 188

$$\begin{aligned} \mathcal{E}_{p_\theta}(a_t | q, d, a_{<t}) &:= \sum_{u, v \in \mathcal{V}} P(E_u)P(E_v)k(E_u, E_v) + \sum_{u, v \in \mathcal{V}} Q(E_u)Q(E_v)k(E_u, E_v) \\ &\quad - 2 \sum_{u, v \in \mathcal{V}} P(E_u)Q(E_v)k(E_u, E_v). \end{aligned} \quad (6)$$

189 We adopt the cosine kernel:
 190

$$k_{\text{cos}}(E_u, E_v) := \frac{1}{2} \left(1 + \frac{E_u^T E_v}{\|E_u\|_2 \|E_v\|_2} \right). \quad (7)$$

191 Note that the cosine kernel acts equivalent to computing cosine similarity between two token
 192 embeddings, which is commonly used to measure the semantic similarity of two pieces of text. In
 193 Section 4.4, we experiment with alternative kernels such as the Gaussian kernel, and we show that
 194 our method is not sensitive to the choice of kernels.
 195

204 3.2 QUANTIFYING INTERNAL KNOWLEDGE UTILIZATION

205 To quantify the utilization of internal knowledge, we focus on the signals in internal states of an LLM.
 206 Specifically, a transformer-based autoregressive LLM has multiple layers, through which information
 207 is gradually added into a residual stream that flows from the input layer to the output layer, shaping
 208 the output token representation and probability distribution (Geva et al., 2022). Studies have found
 209 that by projecting the hidden state of each layer to the token representation space, we can interpret
 210 what an LLM believes after the process of each layer (nostalgebraist, 2020). In addition, via logit
 211 lens (nostalgebraist, 2020), studies have identified the saturation event in an LLM, *i.e.*, the top- k
 212 prediction of the LLM remains constant in all subsequent layers after a certain layer called the k -th
 213 saturation layer (Geva et al., 2022; Lioubashevski et al., 2025).
 214

215 Inspired by these observations, we propose a metric that quantifies how actively the model updates its
 216 predictions across layers. Formally, we define the rate of information processing below.
 217

216 **Definition 3.2 (Information processing rate).** Given an LLM p_θ with L layers, which takes $x_{<t}$ as
 217 the input and generate the next token x_t , we denote $x_{t,1} := \arg \max_v p_\theta(v|x_{<t})$ as the most probable
 218 next token and $h_{t,l} \in \mathbb{R}^D$ as the l -th layer hidden state when generating x_t . Let $f : \mathbb{R}^D \rightarrow \mathcal{P}$ be a
 219 projection from a hidden state to a probability distribution over the vocabulary \mathcal{V} . The information
 220 processing rate of p_θ conditioned on $x_{<t}$ is defined as

$$221 \quad \mathcal{R}_{p_\theta}(x_{<t}) := \frac{\sum_{l=1}^{L-1} \left(1 - \min\left\{\frac{[f(h_{t,l})]_{x_{t,1}}}{p_\theta(x_{t,1}|x_{<t})}, 1\right\}\right) \cdot l}{\sum_{l'=1}^{L-1} \frac{l'}{H(f(h_{t,l'}))}}, \quad (8)$$

225 where $H(\cdot)$ is the entropy function, and f is the logit lens (nostalgebraist, 2020) that projects the
 226 hidden state of each layer to logits using the LayerNorm and the unembedding matrix \mathbf{W} , i.e.,

$$227 \quad \text{LogitLens}(h) := \text{LayerNorm}(h)\mathbf{W}, \quad f(\cdot) := \text{Softmax}(\text{LogitLens}(\cdot)). \quad (9)$$

229 Specifically, $\mathcal{R}_{p_\theta}(x_{<t})$ captures two key elements: (1) The numerator measures the extent to which
 230 each layer's prediction for the most probable token differs from the final output, weighted by layer
 231 depth to emphasize later-layer processing. When $\frac{[f(h_{t,l})]_{x_{t,1}}}{p_\theta(x_{t,1}|x_{<t})}$ is small, it indicates the layer has not
 232 yet converged to the final prediction, suggesting active information processing. (2) The denominator
 233 provides adaptive normalization based on each layer's prediction uncertainty (entropy), giving higher
 234 relative weight to layers that exhibit confident, decisive processing patterns. Given this definition, we
 235 attribute the utilization of internal knowledge to the 1st information processing rate and propose the
 236 following measurement:

237 **Measurement 2 (Internal knowledge utilization).** An LLM is considered to be more heavily
 238 utilizing its internal knowledge to generate a_t when it exhibits a higher information processing rate.
 239 Specifically, we propose that the internal knowledge utilization of an LLM to generate a_t given q and
 240 d can be measured as

$$241 \quad \mathcal{I}_{p_\theta}(a_t|q, d, a_{<t}) := \mathcal{R}_{p_\theta}(q, d, a_{<t}). \quad (10)$$

242 3.3 STATISTICAL VALIDATION OF THE MEASUREMENT

244 In this section, we validate the soundness of our approach. Previous work such as Sun et al. (2025b)
 245 primarily verified whether their scores have a causal relationship with hallucination but failed to show
 246 the relationship between the scores and actual external context/internal knowledge utilization. To
 247 address this, we directly assess whether our measurements capture the intended notion of utilization.
 248 Specifically, we derive verifiable implications that must hold if our proposed measurements are valid.
 249 We then use the proposed score to verify these implications with statistical hypothesis testing. If the
 250 proposed score passes all tests, the score reflects the corresponding utilization.

251 **External context utilization.** To validate Measurement 1, we examine the following implications:

253 **H1.** If Measurement 1 is valid, then $\mathcal{E}_{p_\theta}(a_t|q, d, a_{<t}) > \mathcal{E}_{p_\theta}(a'_t|q, \emptyset, a'_{<t})$. That is, generations with
 254 retrieved documents have stronger external context utilization than generations without.
 255 **H2.** If Measurement 1 is valid, then $\mathcal{E}_{p_\theta}(a_t|q_{\text{sum}}, d_{\text{sum}}, a_{<t}) > \mathcal{E}_{p_\theta}(a_t|q_{\text{QA}}, d_{\text{QA}}, a_{<t})$. That is,
 256 summarization tasks should exhibit higher external context utilization than question answering.

257 **Internal knowledge utilization.** To validate Measurement 2, we examine the following:

259 **H3.** If Measurement 2 is valid, then $\mathcal{R}_{p_\theta}^1(q, \emptyset, a_{<t}) > \mathcal{R}_{p_\theta}^1(q, d, a_{<t})$. That is, generating an answer
 260 without retrieved documents requires more internal knowledge than with retrieved documents.
 261 **H4.** If Measurement 2 is valid, then $\mathcal{R}_{p_\theta}^1(q_{\text{D2T}}, d_{\text{D2T}}, a_{<t}) > \mathcal{R}_{p_\theta}^1(q_{\text{sum}}, d_{\text{sum}}, a_{<t})$. In other words,
 262 data-to-text generation requires more internal knowledge than summarization.

263 To examine **H1**, we utilize data in the QA set of RAGTruth (Niu et al., 2024). We use the original data
 264 to compute $\mathcal{E}_{p_\theta}(a_t|q, d, a_{<t})$, and generate additional answers without providing retrieved documents
 265 as a' to compute $\mathcal{E}_{p_\theta}(a'_t|q, \emptyset, a'_{<t})$. For **H2**, we utilize the Summary and QA set of RAGTruth; for **H4**,
 266 the Summary and Data2Text set; and for **H3**, the entire RAGTruth dataset. We test the hypotheses
 267 with four different instruction-tuned LLMs, including Llama2-7B, 13B (Llama Team, 2023),
 268 Llama3-8B (Llama Team, 2024), and Mistral-7B (Jiang et al., 2023). Results in Table 1 indicate that
 269 all four implications reject their null hypothesis, validating our measurements for external context
 utilization and internal knowledge utilization.

270 Table 1: **All the hypotheses pass the statistical tests.** For H1, H2, H4, we report one-tailed t-statistic;
 271 for H3, we report paired-sample one-tailed t-statistic. All four implications reject their null hypothesis,
 272 validating the soundness of LUMINA. Note that the tests are run with $> 65k$ tokens and the magnitude
 273 of the t-statistic means how easy we can distinguish the two distributions. * $p < 0.05$; ** $p < 0.01$;
 274 *** $p < 0.001$.

LLM	H1	H2	H3	H4
Llama2-7B	79.85***	27.67***	101.20***	15.36***
Llama2-13B	73.49***	20.51***	91.00***	7.71***
Llama3-8B	94.15***	6.35***	102.44***	15.85***
Mistral-7B	88.70***	6.21***	109.26***	9.69***

4 EXPERIMENTS

4.1 EXPERIMENTAL SETTINGS

Baselines. We compare LUMINA with baselines across 8 different hallucination detection strategies: (1) **Uncertainty-based**, which detects hallucination by estimating uncertainty via token-level probability or entropy. Baselines of this category include Perplexity (Ren et al., 2023), LN-Entropy (Malinin & Gales, 2021), and Focus (Zhang et al., 2023). (2) **Cross-sample consistency**, which detects hallucination by sampling multiple responses for a query and measuring their (logic/semantic) consistency. Approaches include SelfCKGPT (Manakul et al., 2023) and EigenScore (Chen et al., 2024). (3) **Verbalization**, which detects hallucinations by prompting another LLM to score the correctness of the answer. Approaches include P(True) (Kadavath et al., 2022) and RefChecker (Hu et al., 2024). (4) **Utilization of external context and internal knowledge**, which decouples these two signals via findings in the study of mechanistic interpretability. Baseline of this category is ReDeEP (Sun et al., 2025b). Details of each baseline are introduced in Appendix B.

LLMs. To demonstrate the generalizability of LUMINA, we conduct experiments with four open-sourced LLMs, including Llama2-{7B, 13B}, Llama3-8B, and Mistral-7B. Specifically, each LLM is used to detect hallucinations in responses generated by the same model. We also report the performance of proxy LLM setting, *i.e.*, using one LLM to detect hallucinations in responses generated by another model, in Sec. 4.3. All LLMs are the instruction-tuned version.

Datasets. Experiments are conducted on two representative RAG hallucination detection benchmarks: **RAGTruth** (Niu et al., 2024), the first high-quality RAG hallucination detection dataset, consisting of three types of RAG tasks, including question answering, data-to-text writing, and news summarization. **HalluRAG** (Ridder & Schilling, 2025), a dataset of free-form question answering in an RAG setting. Details of these datasets are introduced in Appendix C.

Evaluation metrics. We measure the performance with three metrics: **AUROC**, **AUPRC**, and **Pearson’s correlation coefficient** (PCC). AUPRC captures precision-recall trade-offs, while AUROC evaluates the trade-offs between true and false positive rates. These metrics are threshold-agnostic and better suited for comparing scoring-based methods. We also report the optimal precision, recall, and F1 score (Prec_{Opt} , $\text{Recall}_{\text{Opt}}$, F1_{Opt}) in Appendix E.1, where F1_{Opt} is the optimal F1 score among all possible threshold and Prec_{Opt} and $\text{Recall}_{\text{Opt}}$ are corresponding Precision and Recall.

Implementation details. We adopt $\lambda = 0.5$ to compute Eq. (1) as ablations show that balancing the scores of external context and internal knowledge yields relatively strong performance (see Appendix E.3 for detailed ablations). Other implementation details and computational resources of LUMINA are reported in Appendix D and G, respectively.

4.2 MAIN RESULTS

LUMINA achieves state-of-the-art performance. Table 2 summarizes the experimental comparison across methods. The results show that LUMINA has a consistently high performance across datasets and LLMs. In particular, it almost always outperforms ReDeEP, the previous attempt of

324 Table 2: **LUMINA consistently achieves a high performance across datasets and LLMs.** The
 325 highest scores are set in **bold**. Note that HalluRAG dataset does not contain responses generated by
 326 Llama3-8B.

328 329 330 331 332 333 334 335 336 337 338 339 340 341 342 343 344 345 346	328 329 330 331 332 333 334 335 336 337 338 339 340 341 342 343 344 345 346	328 329 330 331 332 333 334 335 336 337 338 339 340 341 342 343 344 345 346	RAGTruth			HalluRAG				
			328 329 330 331 332 333 334 335 336 337 338 339 340 341 342 343 344 345 346	328 329 330 331 332 333 334 335 336 337 338 339 340 341 342 343 344 345 346	328 329 330 331 332 333 334 335 336 337 338 339 340 341 342 343 344 345 346	328 329 330 331 332 333 334 335 336 337 338 339 340 341 342 343 344 345 346	328 329 330 331 332 333 334 335 336 337 338 339 340 341 342 343 344 345 346	328 329 330 331 332 333 334 335 336 337 338 339 340 341 342 343 344 345 346		
347 348 349 350 351 352 353 354 355	347 348 349 350 351 352 353 354 355	347 348 349 350 351 352 353 354 355	Perplexity	0.5103	-0.0118	0.4836	0.4610	-0.0673	0.2332	
			LN-Entropy	0.6964	0.3318	0.6615	0.9102	0.5133	0.6812	
			Focus	0.5633	0.0811	0.5386	0.5652	0.2415	0.3844	
			SelfCKGPT	0.4787	-0.0279	0.4859	0.4669	-0.0070	0.2377	
			Llama2-7B	EigenScore	0.5454	0.0717	0.5183	0.6720	0.2705	0.4470
			P(True)	0.5197	0.0404	0.5334	0.5847	0.1143	0.2976	
			RefChecker	0.5869	0.1751	0.6827	0.4907	-0.0255	0.2750	
			ReDeEP	0.7273	0.3859	0.6971	0.6771	0.1468	0.3378	
			LUMINA	0.7646	0.4546	0.7491	0.9153	0.6554	0.7572	
356 357 358 359 360 361 362 363 364	356 357 358 359 360 361 362 363 364	356 357 358 359 360 361 362 363 364	Perplexity	0.4539	-0.1020	0.3993	0.2548	-0.2366	0.0944	
			LN-Entropy	0.7677	0.4446	0.6838	0.7826	0.3262	0.3567	
			Focus	0.5451	0.0130	0.4603	0.6739	0.2563	0.3181	
			SelfCKGPT	0.4545	-0.0835	0.4106	0.7729	0.2640	0.3029	
			Llama2-13B	EigenScore	0.6329	0.2080	0.5202	0.7862	0.4250	0.4867
			P(True)	0.7543	0.3821	0.7418	0.6914	0.2480	0.2146	
			RefChecker	0.6363	0.2723	0.6988	0.5670	0.1390	0.3169	
			ReDeEP	0.8055	0.5195	0.7792	0.7645	0.2705	0.3001	
			LUMINA	0.8569	0.6041	0.8436	0.9166	0.6044	0.8497	
365 366 367 368 369 370 371 372 373	365 366 367 368 369 370 371 372 373	365 366 367 368 369 370 371 372 373	Perplexity	0.7130	0.3568	0.7183	-	-	-	
			LN-Entropy	0.7072	0.3500	0.7109	-	-	-	
			Focus	0.5258	0.0375	0.5380	-	-	-	
			SelfCKGPT	0.5339	0.0491	0.5550	-	-	-	
			Llama3-8B	EigenScore	0.6001	0.1774	0.5824	-	-	-
			P(True)	0.5407	0.0928	0.5502	-	-	-	
			RefChecker	0.5718	0.1494	0.6874	-	-	-	
			ReDeEP	0.7495	0.4458	0.7817	-	-	-	
			LUMINA	0.7446	0.4236	0.7874	-	-	-	
374 375 376 377 378 379 380 381 382	374 375 376 377 378 379 380 381 382	374 375 376 377 378 379 380 381 382	Perplexity	0.6200	0.1463	0.6106	0.5362	-0.0264	0.1261	
			LN-Entropy	0.7607	0.4386	0.7377	0.9188	0.6076	0.7347	
			Focus	0.7803	0.4188	0.7647	0.8565	0.4318	0.4219	
			SelfCKGPT	0.5680	0.0812	0.5698	0.8275	0.5552	0.6098	
			Mistral-7B	EigenScore	0.5642	0.1006	0.5637	0.8652	0.6411	0.7337
			P(True)	0.7530	0.4334	0.7494	0.5899	0.0886	0.1771	
			RefChecker	0.6017	0.2047	0.7303	0.5065	0.0153	0.1784	
			ReDeEP	0.7615	0.4613	0.8133	0.7870	0.2611	0.3516	
			LUMINA	0.7685	0.4623	0.7942	0.9899	0.7529	0.9431	

365 measuring the utilization of external context and internal knowledge to detect hallucinations. The
 366 gap between them is particularly large on the HalluRAG dataset. Noticeably, LUMINA achieves
 367 more than 0.9 AUROC on the HalluRAG dataset across models, outperforming the baselines by
 368 a substantial margin. We further conduct an error analysis to see when and why LUMINA fails.
 369 Specifically, we sample 20 false-negative and 20 false-positive cases from the RAGTruth dataset,
 370 respectively, and qualitatively analyze the reason of errors. The result reveals that most of the errors
 371 stem from incorrect labels and low-quality retrieved documents of the dataset, suggesting a potentially
 372 higher performance in a setting with high-quality data. The details of this analysis can be found in
 373 Appendix F.

374 **Comparison with supervised approach.** We also compare LUMINA with SAPLMA (Azaria &
 375 Mitchell, 2023), a supervised approach that trained a binary classifier on the last token hidden states
 376 to detect hallucination. Since our method is unsupervised in nature and does not rely on labeled data,
 377 the supervised baseline can be viewed as a performance upper bound. Results in Appendix E.2 show

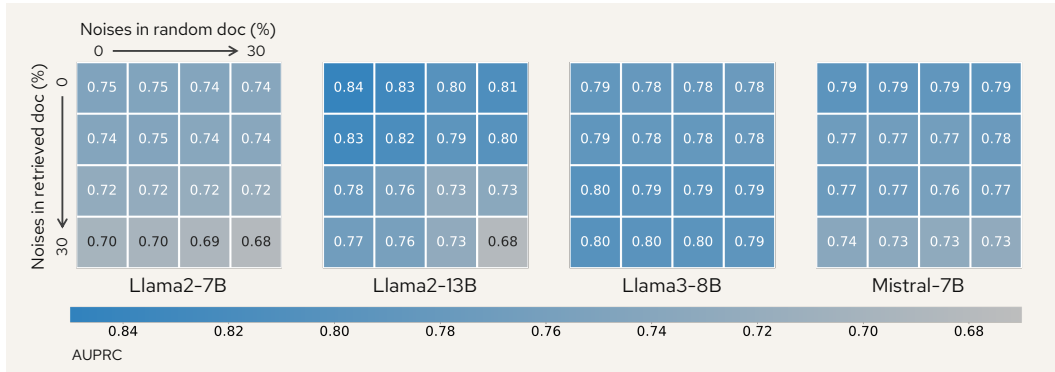


Figure 2: **Noises in context do not largely degrade the performance of LUMINA.** We add $0 \sim 30\%$ noises to the retrieved documents and random documents and evaluate the hallucination detection performance. The experiment is conducted on the RAGTruth dataset.

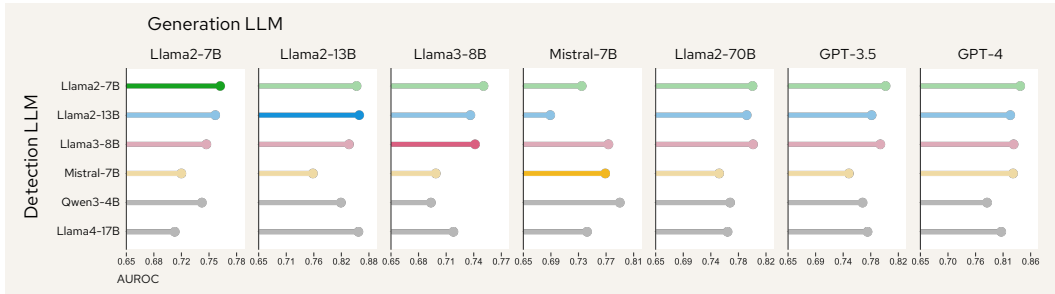


Figure 3: **The “same LLM” setting is not essential for LUMINA to achieve the optimal performance.** On the RAGTruth dataset, for each set of responses generated by the same LLM, we apply LUMINA with a different base LLM to detect hallucination. Bars in more saturated shades indicate settings where the same LLM is used for both generation and detection.

that LUMINA achieves a competitive performance against SAPLMA and even sometimes outperforms it, all without any training, highlighting both its supreme performance and ease of deployment.

4.3 RELAXING ASSUMPTIONS

In Section 3, we implicitly make two assumptions: 1) **perfect context assumption**: we assume the retrieved documents d are correct, sufficient, and relevant to the query. 2) **same LLM assumption**: we assume the LLM used to compute the external context score and internal knowledge score is the same as the LLM used to generate responses. These two assumptions are usually introduced in other hallucination detection works as well (Zhang et al., 2023; Sun et al., 2025b). Unfortunately, they are often strong and have a significant impact on the performance, limiting the usability of these methods (such as for open-sourced model-generated responses only). In this section, we investigate the performance of LUMINA when relaxing these two assumptions, showing the robustness of LUMINA.

Relaxing perfect context assumption. We relax this assumption by gradually injecting noise into the retrieved documents d and random documents d' . Specifically, for the assumption on retrieved documents, we randomly remove $\{0\%, 10\%, 20\%, 30\%\}$ sentences from d . And for the assumption on the random documents, we randomly add $\{0\%, 10\%, 20\%, 30\%\}$ sentences from d to d' . Figure 2 shows the AUPRC of all noise injection combinations on the RAGTruth dataset. The result shows that except Llama2-13B, which has a > 0.1 performance drop after injecting noises, LUMINA with other LLMs yields stable performance. Furthermore, after removing sentences from retrieved documents, LUMINA with Llama3-8B even achieves a higher AUPRC. These results demonstrate the robustness of LUMINA against context noises.

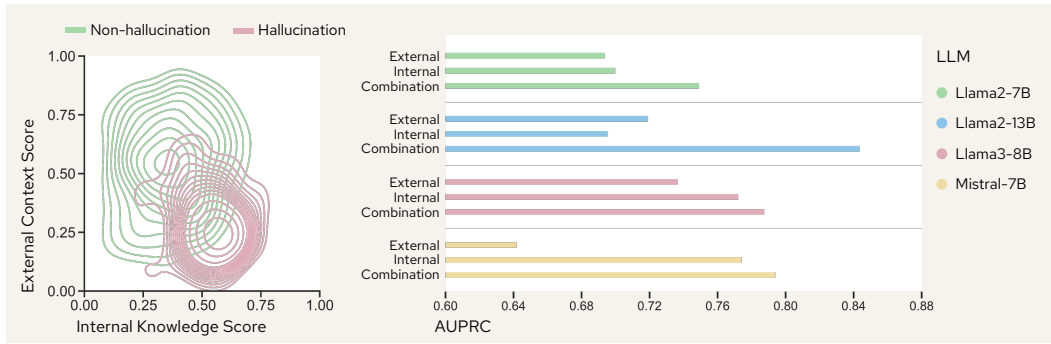


Figure 4: **Combining scores of external context and internal knowledge boosts the hallucination detection performance.** Left: 2D kernel density estimation (KDE) of the distribution of external context score and internal knowledge score of Llama2-13B responses on the RAGTruth dataset. Right: Hallucination detection performance with external/internal score only, as well as the performance of their combination.

Relaxing the same LLM assumption. We relax this assumption by using different LLMs to compute the scores for a response. Specifically, we use Llama2-7B, Llama2-13B, Llama3-8B, Mistral-7B, [Qwen3-4B](#) (Yang et al., 2025), [Llama4-17B](#) (MetaAI, 2025) to detect hallucination on the RAGTruth dataset, which contains responses generated by Llama2-7B, Llama2-13B, Llama2-70B, Llama3-8B, Mistral-7B, GPT-3.5, and GPT-4. Figure 3 shows AUROC across different generator-detector LLM pairs.

The results show that the same model setting is not always necessary. Specifically, Llama2-7B achieves a comparable or higher AUROC than Llama3-8B on Llama3-8B responses. Moreover, LUMINA with Llama2-7B and Llama3-8B has stable performance across different generation LLMs. **In addition, newer models, such as Qwen3-4B and Llama4-17B, also perform well across generation LLMs.** Overall, LUMINA demonstrates a plausible solution for generation LLM-agnostic hallucination detection, which is more practical in real-world scenarios.

4.4 ABLATION STUDY

Impact of kernel selection. We ablate on the selection of kernel $k \in \{\text{Cosine}, \text{RBF}_{0.5}, \text{RBF}_{0.7}, \text{RBF}_1, \text{RBF}_2, \text{RBF}_3\}$, where RBF_σ is a RBF kernel, *i.e.*, $\text{RBF}_\sigma(E_u, E_v) := \exp\left(-\frac{\|E_u - E_v\|_2^2}{2\sigma^2}\right)$. Figure 5 shows the AUPRC of different kernels on the RAGTruth dataset. The results show that the optimal setting of the RBF kernel has a similar performance to the cosine kernel, suggesting our external context score is insensitive to the kernel selection. We default to the cosine kernel as it is less dependent on hyperparameters, making it easy to use in practice.

Impact of external context & internal knowledge. Our final hallucination score is the combination of the external context score and internal knowledge score. To obtain more insights into how each component contributes to the final score, we ablate on the components by considering only the external context score and internal knowledge score. The right plot of Figure 4 shows that combining scores of external context and internal knowledge achieves the highest AUPRC on the RAGTruth dataset for every LLM. For example, on Llama2-13B, the combination leads to more than 10% improvement. This observation justifies the effectiveness of the hallucination score introduced in Definition 2.1. In addition, the left plot of Figure 4 shows that a response generated by Llama2-13B is more likely to be hallucination if it has a high internal knowledge score and a low external context

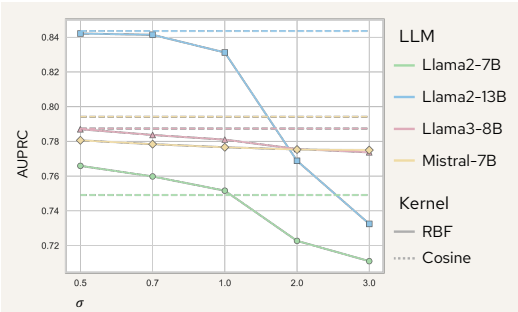


Figure 5: **MMD with cosine kernel performs similarly or better than with RBF kernel.**

486 score. This observation validates Conjecture 1 and suggests that Eq. (1) does not imply an objective
 487 function that forces LLM only using external context to answer questions. Instead, it suggests that
 488 the internal knowledge utilization should be grounded in an external context to achieve a reliable
 489 generation, implying its potential for generalizing to reasoning-intensive tasks.
 490

491 **Additional ablations.** We also conduct other ablations, covering the selection of λ in Eq (1),
 492 the impact of random documents d' , and the contribution of two components of the information
 493 processing rate. Please see Appendix E.3 and E.4 for more details.
 494

495 5 CONCLUSION

496 In this paper, we introduce LUMINA, a novel approach to quantify the utilization of external context
 497 and internal knowledge. These context–knowledge signals provide a principled way to assess
 498 how LLMs balance retrieved evidence against their own parametric knowledge during generation.
 499 Experimental results on common benchmarks across four LLMs demonstrate that LUMINA has a
 500 consistently high performance on hallucination detection for RAG-based generations, outperforming
 501 prior attempts of quantifying external context and internal knowledge utilization, and being com-
 502 petitive with supervised hallucination detection models. Analyses also show that LUMINA is robust
 503 against noise in retrieved documents and can be generalized to the proxy LLM setting, demonstrating
 504 its usability in real-world scenarios.
 505

506 507 ETHICS STATEMENT

508 This work introduces LUMINA, a novel way to estimate the utilization of external context and internal
 509 knowledge when an LLM generates responses with the RAG setup. LUMINA significantly improves
 510 the performance of hallucination detection, which will help increase the reliability of RAG systems
 511 in real-world deployments and reduce the risk of sharing misinformation. Through a deeper analysis
 512 of LUMINA in the future, researchers may better understand how LLMs utilize external context and
 513 internal knowledge to generate responses. Such findings will help the community design approaches
 514 to mitigate hallucinations and create a more reliable AI system.
 515

516 517 REPRODUCIBILITY STATEMENT

518 We provide all details of the implementation of LUMINA in Appendix D, including the approximation
 519 of MMD, the selection of kernel, and the choice of random documents for measuring external context
 520 score, as well as the calibration of internal knowledge score. In Sec. 4.1, we illustrate the experimental
 521 settings, including baselines, datasets, LLMs, and evaluation metrics. The details of baselines and
 522 datasets are further provided in Appendix B and C, respectively. Furthermore, we provide the
 523 codebase of LUMINA at <https://anonymous.4open.science/r/LUMINA-E71B>. These
 524 comprehensive reports will help future studies easily reproduce our experiments.
 525

526 527 BIBLIOGRAPHY

528 Amos Azaria and Tom Mitchell. The internal state of an LLM knows when it’s lying. In *Findings of*
 529 *the Association for Computational Linguistics: EMNLP 2023*, 2023.

530 Chao Chen, Kai Liu, Ze Chen, Yi Gu, Yue Wu, Mingyuan Tao, Zhihang Fu, and Jieping Ye. INSIDE:
 531 LLMs’ internal states retain the power of hallucination detection. In *The Twelfth International*
 532 *Conference on Learning Representations*, 2024.

533 Wenqi Fan, Yujuan Ding, Liangbo Ning, Shijie Wang, Hengyun Li, Dawei Yin, Tat-Seng Chua, and
 534 Qing Li. A survey on rag meeting llms: Towards retrieval-augmented large language models. In
 535 *Proceedings of the 30th ACM SIGKDD Conference on Knowledge Discovery and Data Mining*,
 536 KDD ’24, pp. 6491–6501, 2024. ISBN 9798400704901.

540 Yunfan Gao, Yun Xiong, Xinyu Gao, Kangxiang Jia, Jinliu Pan, Yuxi Bi, Yi Dai, Jiawei Sun, Meng
 541 Wang, and Haofen Wang. Retrieval-augmented generation for large language models: A survey.
 542 *arXiv preprint arXiv:2312.10997*, 2024.

543

544 Mor Geva, Avi Caciularu, Kevin Wang, and Yoav Goldberg. Transformer feed-forward layers build
 545 predictions by promoting concepts in the vocabulary space. In *Proceedings of the 2022 Conference*
 546 *on Empirical Methods in Natural Language Processing*, pp. 30–45, 2022.

547

548 Arthur Gretton, Karsten M. Borgwardt, Malte J. Rasch, Bernhard Schölkopf, and Alexander Smola.
 549 A kernel two-sample test. *Journal of Machine Learning Research*, 13(25):723–773, 2012. ISSN
 550 1533-7928.

551

552 Jiatong Han, Jannik Kossen, Muhammed Razzak, Lisa Schut, Shreshth A Malik, and Yarin Gal.
 553 Semantic entropy probes: Robust and cheap hallucination detection in llms. In *ICML 2024*
 554 *Workshop on Foundation Models in the Wild*, 2024.

555

556 Xiangkun Hu, Dongyu Ru, Lin Qiu, Qipeng Guo, Tianhang Zhang, Yang Xu, Yun Luo, Pengfei Liu,
 557 Yue Zhang, and Zheng Zhang. Refchecker: Reference-based fine-grained hallucination checker
 558 and benchmark for large language models. *arXiv preprint arXiv:2405.14486*, 2024.

559

560 Lei Huang, Weijiang Yu, Weitao Ma, Weihong Zhong, Zhangyin Feng, Haotian Wang, Qianglong
 561 Chen, Weihua Peng, Xiaocheng Feng, Bing Qin, and Ting Liu. A survey on hallucination in large
 562 language models: Principles, taxonomy, challenges, and open questions. *ACM Trans. Inf. Syst.*,
 563 2024. ISSN 1046-8188.

564

565 Albert Q. Jiang, Alexandre Sablayrolles, Arthur Mensch, Chris Bamford, Devendra Singh Chaplot,
 566 Diego de las Casas, Florian Bressand, Gianna Lengyel, Guillaume Lample, Lucile Saulnier,
 567 Lélio Renard Lavaud, Marie-Anne Lachaux, Pierre Stock, Teven Le Scao, Thibaut Lavril, Thomas
 568 Wang, Timothée Lacroix, and William El Sayed. Mistral 7b. *arXiv preprint arXiv:2310.06825*,
 569 2023.

570

571 Saurav Kadavath, Tom Conerly, Amanda Askell, Tom Henighan, Dawn Drain, Ethan Perez, Nicholas
 572 Schiefer, Zac Hatfield-Dodds, Nova DasSarma, Eli Tran-Johnson, Scott Johnston, Sheer El-Showk,
 573 Andy Jones, Nelson Elhage, Tristan Hume, Anna Chen, Yuntao Bai, Sam Bowman, Stanislav Fort,
 574 Deep Ganguli, Danny Hernandez, Josh Jacobson, Jackson Kernion, Shauna Kravec, Liane Lovitt,
 575 Kamal Ndousse, Catherine Olsson, Sam Ringer, Dario Amodei, Tom Brown, Jack Clark, Nicholas
 576 Joseph, Ben Mann, Sam McCandlish, Chris Olah, and Jared Kaplan. Language models (mostly)
 577 know what they know. *arXiv preprint arXiv:2207.05221*, 2022.

578

579 Daliang Li, Ankit Singh Rawat, Manzil Zaheer, Xin Wang, Michal Lukasik, Andreas Veit, Felix Yu,
 580 and Sanjiv Kumar. Large language models with controllable working memory. In *Findings of the*
 581 *Association for Computational Linguistics: ACL 2023*, 2023.

582

583 Daria Lioubashevski, Tomer Schlank, Gabriel Stanovsky, and Ariel Goldstein. Looking beyond
 584 the top-1: Transformers determine top tokens in order. In *Proceedings of the 42nd International*
 585 *Conference on Machine Learning*, 2025.

586

587 AI @ Meta Llama Team. Llama 2: Open foundation and fine-tuned chat models. *arXiv preprint*
 588 *arXiv:2307.09288*, 2023.

589

590 AI @ Meta Llama Team. The llama 3 herd of models. *arXiv preprint arXiv:2407.21783*, 2024.

591

592 Shayne Longpre, Kartik Perisetla, Anthony Chen, Nikhil Ramesh, Chris DuBois, and Sameer Singh.
 593 Entity-based knowledge conflicts in question answering. In *Proceedings of the 2021 Conference*
 594 *on Empirical Methods in Natural Language Processing*, 2021.

595

596 Junliang Luo, Tianyu Li, Di Wu, Michael R. M. Jenkin, Steve Liu, and Gregory Dudek. Hallucination
 597 detection and hallucination mitigation: An investigation. *arXiv preprint arXiv:2401.08358*, 2024.

598

599 Andrey Malinin and Mark Gales. Uncertainty estimation in autoregressive structured prediction. In
 600 *International Conference on Learning Representations*, 2021.

594 Potsawee Manakul, Adian Liusie, and Mark Gales. SelfCheckGPT: Zero-resource black-box hallucination
 595 detection for generative large language models. In *Proceedings of the 2023 Conference on Empirical Methods in Natural Language Processing*, 2023.

596

597 MetaAI. Llama-4-Scout-17B-16E-Instruct. <https://huggingface.co/meta-llama/Llama-4-Scout-17B-16E-Instruct>, 2025.

598

599

600 Cheng Niu, Yuanhao Wu, Juno Zhu, Siliang Xu, KaShun Shum, Randy Zhong, Juntong Song, and
 601 Tong Zhang. RAGTruth: A hallucination corpus for developing trustworthy retrieval-augmented
 602 language models. In *Proceedings of the 62nd Annual Meeting of the Association for Computational
 603 Linguistics (Volume 1: Long Papers)*, 2024.

604

605 nostalgebraist. interpreting gpt: the logit lens, 2020. URL <https://www.lesswrong.com/posts/AcKRB8wDpdaN6v6ru/interpreting-gpt-the-logit-lens>.

606

607 Seongheon Park, Xuefeng Du, Min-Hsuan Yeh, Haobo Wang, and Yixuan Li. Steer LLM latents for
 608 hallucination detection. In *Forty-second International Conference on Machine Learning*, 2025.

609

610 Jie Ren, Jiaming Luo, Yao Zhao, Kundan Krishna, Mohammad Saleh, Balaji Lakshminarayanan, and
 611 Peter J Liu. Out-of-distribution detection and selective generation for conditional language models.
 612 In *The Eleventh International Conference on Learning Representations*, 2023.

613

614 Fabian Ridder and Malte Schilling. The hallurag dataset: Detecting closed-domain hallucinations in
 615 rag applications using an llm's internal states. *arXiv preprint arXiv:2412.17056*, 2025.

616

617 Kurt Shuster, Spencer Poff, Moya Chen, Douwe Kiela, and Jason Weston. Retrieval augmentation
 618 reduces hallucination in conversation. In *Findings of the Association for Computational Linguistics: EMNLP 2021*, 2021.

619

620 Kaiser Sun, Fan Bai, and Mark Dredze. What is seen cannot be unseen: The disruptive effect of
 621 knowledge conflict on large language models. *arXiv preprint arXiv:2506.06485*, 2025a.

622

623 ZhongXiang Sun, Xiaoxue Zang, Kai Zheng, Jun Xu, Xiao Zhang, Weijie Yu, Yang Song, and Han Li.
 624 RedeEP: Detecting hallucination in retrieval-augmented generation via mechanistic interpretability.
 625 In *The Thirteenth International Conference on Learning Representations*, 2025b.

626

627 Yufei Tao, Adam Hiatt, Rahul Seetharaman, and Ameeta Agrawal. "lost-in-the-later": Framework
 628 for quantifying contextual grounding in large language models. *arXiv preprint arXiv:2507.05424*,
 629 2025.

630

631 Lei Wang. Seredep: Hallucination detection in retrieval-augmented models via semantic entropy
 632 and context-parameter fusion. *arXiv preprint arXiv:2505.07528*, 2025.

633

634 Rongwu Xu, Zehan Qi, Zhijiang Guo, Cunxiang Wang, Hongru Wang, Yue Zhang, and Wei Xu.
 635 Knowledge conflicts for LLMs: A survey. In Yaser Al-Onaizan, Mohit Bansal, and Yun-Nung
 636 Chen (eds.), *Proceedings of the 2024 Conference on Empirical Methods in Natural Language
 637 Processing*, 2024.

638

639 Khurram Yamin, Gaurav Ghosal, and Bryan Wilder. Llms struggle to perform counterfactual
 640 reasoning with parametric knowledge. *arXiv preprint arXiv:2506.15732*, 2025.

641

642 An Yang, Anfeng Li, Baosong Yang, Beichen Zhang, Binyuan Hui, Bo Zheng, Bowen Yu, Chang
 643 Gao, Chengan Huang, Chenxu Lv, Chujie Zheng, Dayiheng Liu, Fan Zhou, Fei Huang, Feng Hu,
 644 Hao Ge, Haoran Wei, Huan Lin, Jialong Tang, Jian Yang, Jianhong Tu, Jianwei Zhang, Jianxin
 645 Yang, Jiaxi Yang, Jing Zhou, Jingren Zhou, Junyang Lin, Kai Dang, Keqin Bao, Kexin Yang,
 646 Le Yu, Lianghao Deng, Mei Li, Mingfeng Xue, Mingze Li, Pei Zhang, Peng Wang, Qin Zhu, Rui
 647 Men, Ruize Gao, Shixuan Liu, Shuang Luo, Tianhao Li, Tianyi Tang, Wenbiao Yin, Xingzhang
 648 Ren, Xinyu Wang, Xinyu Zhang, Xuancheng Ren, Yang Fan, Yang Su, Yichang Zhang, Yinger
 649 Zhang, Yu Wan, Yuqiong Liu, Zekun Wang, Zeyu Cui, Zhenru Zhang, Zhipeng Zhou, and Zihan
 650 Qiu. Qwen3 technical report. *arXiv preprint arXiv:2505.09388*, 2025.

651

652 Tianhang Zhang, Lin Qiu, Qipeng Guo, Cheng Deng, Yue Zhang, Zheng Zhang, Chenghu Zhou,
 653 Xinbing Wang, and Luoyi Fu. Enhancing uncertainty-based hallucination detection with stronger
 654 focus. In *Proceedings of the 2023 Conference on Empirical Methods in Natural Language
 655 Processing*, 2023.

APPENDIX

CONTENTS

648	A Broader Impacts	13
649		
650		
651	B Details of Baselines	13
652		
653	C Details of Datasets	14
654		
655	D Implementation Details of LUMINA	14
656		
657	E Additional Experimental Results	15
658		
659	E.1 Evaluation with Other Metrics	15
660		
661	E.2 Compare with supervised baselines	16
662		
663	E.3 Performance with Hyperparameter Tuning	16
664		
665	E.4 Additional Ablation study	17
666		
667	F Error Analysis	17
668		
669	G Computational Resources	18
670		
671		
672		
673		
674		
675		
676		
677		

A BROADER IMPACTS

Beyond hallucination detection, LUMINA has broader impacts in interpretability and LLM understanding. Specifically, our proposed score validation framework in Sec. 3.3 suggests a novel way to empirically validate the finding of mechanistic interpretability, which can be used to highlight the soundness of proposed hypotheses. In addition, our proposed information processing rate in Sec. 3.2 presents a new lens for examining the internal states of LLMs. Deeper investigation of this measure could help the community better characterize how LLMs reason and leverage internal knowledge, potentially leading to more reliable training and inference processes. While our experiments focus on using LUMINA for hallucination detection, its utility extends further. For instance, it could inform the design of new training objectives or decoding algorithms aimed at mitigating hallucinations, ultimately making LLMs more reliable and trustworthy.

B DETAILS OF BASELINES

(1) Token-level uncertainty:

- **Perplexity:** This approach measured the perplexity of the generated response as uncertainty and to detect hallucinations.
- **LN-Entropy:** This approach measured sequence-level uncertainty with entropy normalized by sequence length. A higher entropy indicates greater uncertainty and a higher likelihood of hallucinations.
- **Focus:** This approach used entropy and token probability as a based score, and calibrated it by focusing only on key informative tokens and propagating the score according to the attention weight.

(2) Cross-sample consistency:

- 702 • **SelfCKGPT:** This approach sampled multiple responses and used an NLI model to check the
 703 logistic consistency between the target generation and additional samples. In our experiment,
 704 we follow the setting of [Manakul et al. \(2023\)](#) to set the sample size as 20.
- 705 • **EigenScore:** Similar to SelfCKGPT, this approach sampled multiple responses and checked
 706 the semantic consistency between the additional samples and the target generation through
 707 measuring the eigenvalues of responses’ covariance matrix. In our experiment, we set the
 708 sample size as 20.

709
 710 **(3) Verbalization:**

711
 712 • **P(True):** This approach prompted an LLM with the generated answer and asked whether
 713 the LLM think the answer is true. The approach then estimated the probability of the “Yes”
 714 generated by the LLM.

715 • **RefChecker:** This approach prompted an LLM to extract claims from generation, and
 716 prompted another LLM to verify the logical consistency between each claim and reference
 717 documents. In our experiment, we use [dongyru/Mistral-7B-Claim-Extractor](#),
 718 the model finetuned by [Hu et al. \(2024\)](#), to extract claims.

719
 720 **(4) Utilization of external context and internal knowledge:**

721
 722 • **ReDeEP:** For external context utilization, ReDeEP measured the cosine similarity between
 723 the generated token and topK attended tokens in retrieved documents. For internal knowledge
 724 utilization, it measured the JS divergence of the vocabulary distributions between logit lens
 725 outputs before and after FFN layers in a Transformer. At the end, it weighted summed the
 726 two scores to obtain a hallucination score.

727 **C DETAILS OF DATASETS**

728
RAGTruth. The RAGTruth dataset is a human annotated hallucination detection dataset, containing
 729 15,090 training data and 2,700 testing data. Each data point consists of a query, retrieved documents,
 730 LLM-generated answer, and span-level hallucination annotation. The dataset covers three tasks,
 731 including summarization, data to text generation, and question answering. For each query-and-
 732 documents pair, RAGTruth provides answers generated by six different LLMs, including Llama2-7B,
 733 Llama2-13B, Llama2-70B, Mistral-7B, GPT-3.5, and GPT-4. In our experiment, we also utilize the
 734 extended test set provided by [Sun et al. \(2025b\)](#), who curated and annotated Llama3-8B generated
 735 responses.

736
HalluRAG. HalluRAG is an LLM annotated hallucination detection dataset for question answering.
 737 Ridder & Schilling (2025) prompted GPT-4o to generate question given sentences from Wikipedia,
 738 then used Llama2-7B, Llama2-13B, and Mistral-7B to generate answer for each question given
 739 the relevant Wikipedia article. The hallucination labels were assigned by GPT-4o with a Chain-of-
 740 Thought (CoT) prompt and verified by human. HalluRAG contains both answerable and unanswerable
 741 questions, while we only use the answerable instances for evaluation.

742 **D IMPLEMENTATION DETAILS OF LUMINA**

743 For external context utilization, we measure MMD with Eq. (6), which requires summing over the
 744 combinations of the entire vocabulary. In practice we approximate it with the top 100 tokens to
 745 reduce the computational cost. To obtain $p_{\text{ctx}'}$, in our experiment we treat the retrieved documents of
 746 another data point as the d' of the target data point. In a real-world RAG system, d' can be obtained
 747 by selecting random documents from the data store or retrieving less relevant documents of the query
 748 with a retrieval model.

749
 750 For internal knowledge utilization, Eq. (10) computes the first information process rate of generating
 751 a_t based on the next token with the highest probability. However, due to the sampling process of
 752 generation, the generated token a_t is not always the highest probability token. Thus, the internal
 753 knowledge used during the generation process may not fully apply to a_t . To take this factor into

756 **Table 3: LUMINA consistently achieves a balanced precision-recall trade-off and high F1 score**
 757 **across datasets and LLMs.** We report the score of Prec_{Opt} , $\text{Recall}_{\text{Opt}}$, and F1_{Opt} for LUMINA and
 758 baselines on each dataset.

760	761	762	RAGTruth			HalluRAG		
			763	764	765	766	767	768
769	770	771	772	773	774	775	776	777
778	779	780	781	782	783	784	785	786
787	788	789	790	791	792	793	794	795
796	797	798	799	800	801	802	803	804
805	806	807	808	809	810	811	812	813

795 account, we calibrate the internal knowledge score by the ratio of probability between the generated
 796 token and the highest probability token. In the end, the calibrated internal knowledge score of a_t is
 797 defined as

$$\mathcal{I}_{p_{\theta}}(a_t|q, d, a_{<t}) := \frac{p_{\theta}(a_t|q, d, a_{<t})}{p_{\theta}(a_{t,1}|q, d, a_{<t})} \cdot \mathcal{R}_{p_{\theta}}(q, d, a_{<t}). \quad (11)$$

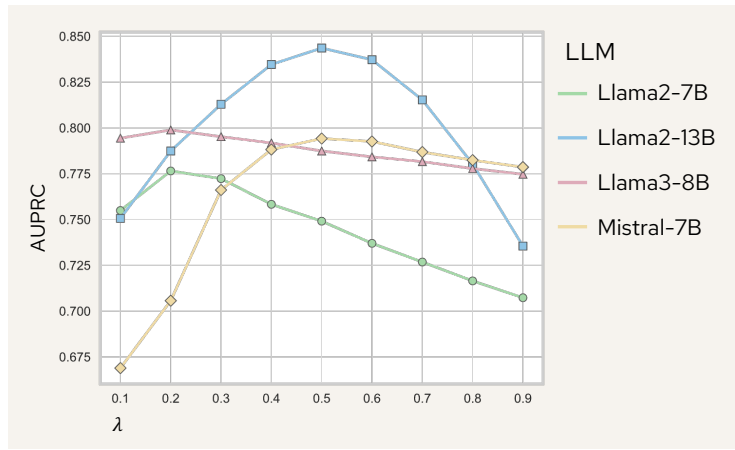
802 E ADDITIONAL EXPERIMENTAL RESULTS

804 E.1 EVALUATION WITH OTHER METRICS

806 Table 3 shows the scores of Prec_{Opt} , $\text{Recall}_{\text{Opt}}$, and F1_{Opt} on each dataset. The results show that LUMINA
 807 consistently has a balanced precision-recall trade-off, where the differences between Prec_{Opt}
 808 and $\text{Recall}_{\text{Opt}}$ are smaller than other baselines. Specifically, it achieves $(\text{Prec}_{\text{Opt}}, \text{Recall}_{\text{Opt}}) =$
 809 $(0.9, 0.9)$ on HalluRAG with Mistral-7B. This suggests that LUMINA does not over-predict hallucinations
 810 to achieve a high F1_{Opt} score.

810
 811 **Table 4: LUMINA achieves a competitive performance against supervised approaches.** We report
 812 the score of AUROC (ROC), Pearson’s correlation coefficient (PCC), and AUPRC (PRC) for LUMINA
 813 and baselines on each dataset. The highest scores are set in **bold**.
 814

815 816 817 818 819 820 821 822 823 824 825 826 827 828 829 830 831 832 833 834 835 836 837 838 839	840 841 842 843 844 845 846 847 848 849 850 851 852 853 854 855 856 857 858 859 860 861 862 863 864 865 866	RAGTruth			HalluRAG				
		840 841 842 843 844 845 846 847 848 849 850 851 852 853 854 855 856 857 858 859 860 861 862 863 864 865 866	840 841 842 843 844 845 846 847 848 849 850 851 852 853 854 855 856 857 858 859 860 861 862 863 864 865 866	840 841 842 843 844 845 846 847 848 849 850 851 852 853 854 855 856 857 858 859 860 861 862 863 864 865 866	840 841 842 843 844 845 846 847 848 849 850 851 852 853 854 855 856 857 858 859 860 861 862 863 864 865 866				
815 816 817 818 819 820 821 822 823 824 825 826 827 828 829 830 831 832 833 834 835 836 837 838 839	840 841 842 843 844 845 846 847 848 849 850 851 852 853 854 855 856 857 858 859 860 861 862 863 864 865 866	Llama2-7B	SAPLMA	0.6508	0.2530	0.6446	0.8813	0.6710	0.8023
		LUMINA	0.7646	0.4546	0.7491	0.9153	0.6554	0.7572	
815 816 817 818 819 820 821 822 823 824 825 826 827 828 829 830 831 832 833 834 835 836 837 838 839	840 841 842 843 844 845 846 847 848 849 850 851 852 853 854 855 856 857 858 859 860 861 862 863 864 865 866	Llama2-13B	SAPLMA	0.8337	0.5623	0.8466	0.8925	0.8249	0.8647
		LUMINA	0.8569	0.6041	0.8436	0.9166	0.6044	0.8497	
815 816 817 818 819 820 821 822 823 824 825 826 827 828 829 830 831 832 833 834 835 836 837 838 839	840 841 842 843 844 845 846 847 848 849 850 851 852 853 854 855 856 857 858 859 860 861 862 863 864 865 866	Mistral-7B	SAPLMA	0.8073	0.5027	0.8164	0.9667	0.7920	0.9088
		LUMINA	0.7685	0.4623	0.7942	0.9899	0.7529	0.9431	



840 **Figure 6: A good performance of LUMINA happens with a medium λ value.** We alter λ in Eq. (1)
 841 to control the weight of internal knowledge score and external context score and evaluate the resulted
 842 hallucination detection performance. We conduct the experiment on the RAGTruth dataset and report
 843 the AUPRC score.
 844
 845

E.2 COMPARE WITH SUPERVISED BASELINES

846 We further compare LUMINA with SAPLMA (Azaria & Mitchell, 2023), a supervised approach that
 847 trained a MLP model over the internal hidden states of the last generated token to classify whether the
 848 generation is hallucination or not. Following the original paper, we use hidden states at the 20th layer
 849 as input features of SAPLMA. Result in Table 4 shows that LUMINA has a competitive performance
 850 against SAPLMA and even sometimes outperforms it. Note that Table 4 doesn’t show the result of
 851 Llama3-8B as the training set doesn’t contain responses generated by Llama3-8B.
 852
 853

E.3 PERFORMANCE WITH HYPERPARAMETER TUNING

854 We evaluate the hallucination detection performance with $\lambda \in \{0.1, 0.2, 0.3, 0.4, 0.5, 0.6, 0.7, 0.8,$
 855 $0.9\}$. Figure 6 shows the AUPRC of different λ on the RAGTruth dataset. The results show that
 856 the LUMINA achieves the optimal performance with varies λ across LLMs. For Llama2-13B and
 857 Mistral-7B, setting $\lambda = 0.5$, *i.e.*, the default setting, is the optimal. While for Llama2-7B and
 858 Llama3-8B, the optimal λ is 0.2. However, for these two models, their performance only drops less
 859 than 0.025 when setting $\lambda = 0.5$, suggesting that weighting internal knowledge and external context
 860 utilization equally is still a good practice.
 861
 862

864
865
866
867
868
869
870
871
872
873
874
875
876
877
878
879
880
881
882
883
884
885
886
887
888
889
890
891
892
893
894
895
896
897
898
899
900
901
902
903
904
905
906
907
908
909
910
911
912
913
914
915
916
917
918

Table 5: **Both components of information processing rate are important.** We report the AUROC of each component, as well as the performance of their combination.

LLM	Layer weighting	Entropy normalization	Both
Llama2-7B	0.7023	0.7164	0.7652
Llama2-13B	0.8007	0.8433	0.8554
Llama3-8B	0.7512	0.7683	0.7697
Mistral-7B	0.6111	0.6723	0.7679

E.4 ADDITIONAL ABLATION STUDY

Impact of MMD approximation. When implementing LUMINA, we approximate MMD with the top k tokens and set $k = 100$, aiming to balance between computational cost and approximation error. To test the impact of k , we ablate on $k \in \{50, 100, 500\}$ and evaluate on the RAGTruth dataset. The result shows a consistent AUROC across different k , with a $< 0.02\%$ difference, suggesting that LUMINA is insensitive to the choice of MMD approximation. Additionally, in cases where the computational power is limited, choosing $k = 50$ is also considerable.

Impact of random documents. In Section 4.3, we study the impact of noises in the retrieved and random documents. To further examine the impact of different random documents on the performance, we select 5 different random documents and use each of them to compute the hallucination score. Experiments on the RAGTruth dataset shows that the standard deviation across the 5 rounds with different random documents is < 0.0025 , suggesting that LUMINA is very robust to the choice of random document.

Impact of the components of the information processing rate. Our proposed information processing rate consist of two components: layer weighting probability ratio (numerator) and entropy normalization (denominator). Table 5 shows the AUROC of ablating these two components. The result shows that both components contribute to the overall performance, justifying our design choice.

F ERROR ANALYSIS

To analyze the failure of LUMINA, we sample 40 cases from the RAGTruth dataset that are (1) hallucinated with high-external context and low-internal knowledge scores (*i.e.*, false negative) or (2) non-hallucinated with low-external context and high-internal knowledge scores (*i.e.*, false positive). We qualitatively analyze these cases and categorize them into three groups:

(1) Incorrect labels. Sometimes LLMs generate fabricated content that is not sourced from the retrieved document (*e.g.*, a detailed menu of a restaurant). However, these fabricated contents are sometimes not identified by human annotators. Also, human annotators sometimes misclassify semantically equivalent content as hallucination. In these cases, the provided labels are incorrect, and LUMINA indeed correctly detects hallucination.

(2) Generally low hallucination score for the summarization task. We observe that many false negative samples come from the summarization task. In these cases, the LLM does generate content that contradicts the retrieved documents and has a relatively high internal knowledge score. However, since most of the generated content is still grounded in the retrieved documents, they usually have a high external score as well, resulting in a relatively low hallucination score. This observation suggests that different tasks might have different distributions of hallucination scores. A better practice is to independently evaluate the hallucination detection performance on each task.

(3) Low quality of retrieved documents. For the false positive cases, we observe that many of them are due to the quality issue of the retrieved documents. These documents often contain only irrelevant information or are too vague to concretely answer the query. Thus, the LLM has to reason over them and respond with “unable to answer” or use its internal knowledge to generate answers with

Table 6: The errors of LUMINA are mainly due to incorrect labels, quality of retrieved documents, and task-dependent biases. We report the proportion of each error type classified by GPT-5.

Error Type	Proportion
False Positive	
Incorrect labels	32%
Low quality of retrieved documents	24%
Others	44%
False Negative	
Incorrect labels	16%
Low hallucination score for summarization task	64%
Others	20%

Table 7: **LUMINA is more efficient than ReDeEP.** We report the average computational time (second/sample) for ReDeEP and LUMINA.

LLM	ReDeEP	LUMINA
Llama2-7B	0.86	0.69
Llama2-17B	1.17	0.88
Llama3-8B	1.13	0.58
Mistral-7B	0.72	0.54

details and examples. This results in a relatively high internal knowledge score and a low external context score. To address this, a future direction can focus on assessing whether the utilization of internal knowledge is necessary and correct, and using that to calibrate the hallucination score.

We extend the error analysis by sampling 50 false positive and 50 false negative cases, and prompting GPT-5 to classify the reason for error. The result in Table 6 shows that while there are edge cases that LUMINA can not handle correctly, many of the errors are due to incorrect labels and low quality of retrieved documents. For those edge cases, we observe that they usually happen when the internal knowledge and external context scores are close and when the task is more reasoning intensive. Thus, when deploying LUMINA, controlling the balance between internal knowledge score and external knowledge score according to the task might be a good practice to further increase the performance.

G COMPUTATIONAL RESOURCES

LUMINA is a lightweight and efficient approach, which requires only two forward passes to obtain the necessary information to compute external context and internal knowledge scores. As LUMINA does not require generating multiple samples nor training, it is easy to scale up to a large amount of data. All the experiments of LUMINA are conducted on a single Nvidia H100 GPU. The execution time of computing both external context and internal knowledge scores varies depending on the length of the response. For responses around 150 tokens, the average computational time is less than 1 second. **In addition, while LUMINA requires two forward passes to compute the score, it is consistently more efficient than ReDeEP, as shown in Table 7.** We believe that it is because for the external context score, ReDeEP has to store the entire attention map for every layer and use that to select the top k tokens from the external context. And for the internal knowledge score, ReDeEP has to apply the logit lens before and after FFN for each transformer layer. In contrast, our external context score only requires approximating MMD at the output layer, and our internal knowledge score needs applying the logit lens only once per layer. These design choices reduce the computational cost, making LUMINA much more efficient.